The first measurements of edge plasma electron temperature by the Thomson scattering method on a TUMAN-3M tokamak

© A.S. Tukachinsky [1], V.V. Vasiliev [2], G.I. Abdullina [1], S.E. Alexandrov [1], L.G. Askinazi [1], A.A. Belokurov [1], N.S. Zhiltsov [1], N.A. Zhubr [1], A.N. Koval [1], V.A. Kornev [1], S.V. Krikunov [1], G.S. Kurskiev [1], S.V. Lebedev [1], D.I. Litvinova [1], E.E. Mukhin [1], D.V. Razumenko [1], V.A. Solovey [1], A.I. Smirnov [1], I.B. Tereshchenko [1], E.E. Tkachenko [1], S.Yu. Tolstyakov [1], L.K. Shuvalova [1]

[1] Ioffe Institute, St. Petersburg, Russia
[2] Peter the Great Saint-Petersburg Polytechnic University, St. Petersburg, Russia
E-mail: Vlad-blode-mag@mail.ru

Received April 28, 2024
Revised July 31, 2024
Accepted October 30, 2024

The results of the first measurements of the electron temperature in edge plasma of the TUMAN-3M tokamak are presented. These results were obtained with a recently installed Thomson scattering diagnostics system. The experiments were performed in 2023 year with test light collecting system set up for observation of plasma in region with $r/a > 0.75$ including $r/a = 0.95$ edge point. The main objective of measurements in this plasma region was to determine sensitivity of the diagnostics in different experimental conditions. The experiments were performed in ohmic discharges in two scenarios: in discharges with LH-transition (working gas — deuterium) and in discharges with gas puffing modulation (working gas — hydrogen).

Keywords: High-temperature plasma, tokamak, Thomson scattering, electron temperature.

DOI: 10.61011/TPL.2024.12.60371.6456k

The interest in measurements of electron temperature T_e in edge plasma is due to the relation between processes at the boundary and in the center of a plasma column and to the need to obtain data on T_e to understand the physics of phenomena observed in edge plasma. For example, the formation of an edge transport barrier may lead to a global improvement in heat and particle confinement (H-mode). Edge measurements of T_e by Thomson diagnostics are complicated by the low electron density in edge plasma (and the corresponding low level of the Thomson scattering signal) and the possible high intensity of probing laser radiation scattered parasitically from the chamber walls.

Thomson scattering diagnostics is based on the analysis of the spectrum of probing laser radiation scattered by free plasma electrons. When radiation is scattered, the spectrum broadens due to the thermal motion of electrons, which makes it possible to determine T_e. The Thomson diagnostic complex (TDC) discussed in this paper has a single-pass geometry with a probing Nd:YAG laser operating at a wavelength of 1064 nm, a pulse repetition rate of 10 Hz, a radiation energy of 1.5 J per pulse, and a pulse duration of 15 ns. The low repetition rate of probing pulses forces one to study the time evolution of T_e by the „shot-to-shot" method in a series of similar discharges with variation of the probing time point. The scattered radiation (SR) spectrum is analyzed by three four-channel polychromators with a high optical transmittance (up to 80%). Radiation is detected in each polychromator channel by an avalanche photodiode with a high quantum yield ($\sim 50\%$ at a wavelength of 1064 nm). A fast analog-to-digital converter with a sampling rate of 5 GHz is used to digitize scattering signals. A similar system for SR recording was described in detail in [1,2]. A specially designed system synchronizing the actuation of the TDC probing laser and the tokamak systems provides an opportunity to perform measurements of the electron temperature at a given moment in time.

At the first stage of the diagnostic complex commissioning an available lens was used, which parameters didn't meet the requirements completely. A temporary SR collection system (Fig. 1, a) was assembled to test its sensitivity and identify possible drawbacks. It consists of a lens and three fiber optic assemblies (hereinafter referred to as bundles) with a rectangular cross section at the input and a round cross section at the output (Fig. 1, b) mounted on a common optical rail. The optical scheme for collecting scattered radiation is configured in such a way that the lens projects a vertical segment of the probing axis in plasma onto a segment in the image plane with a $1/\Gamma = 1/5$ reduction. The input ends of the fiber optic bundles are located within this section: the long side is oriented vertically, and the bundles are brought as close together as possible (as far as the design of their sheathing allows).

The input configuration of the fiber optic assembly is determined by the laser beam shape. To obtain a more intense signal and a better scattered signal/plasma signal ratio, one needs to collect as much scattered light as possible and as little plasma radiation as possible. Since a laser beam may be approximated roughly as a cylinder elongated along the probing axis, a rectangular shape elongated

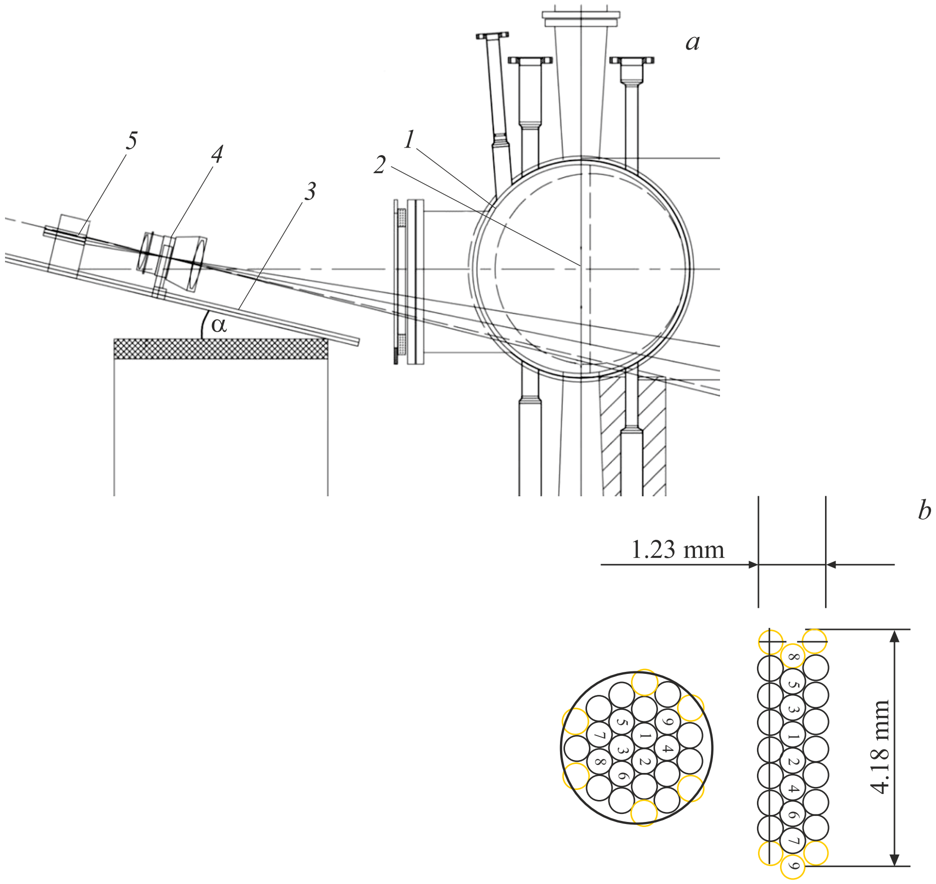

Figure 1. *a* — Diagram of the radiation collection system configured to measure scattering signals from regions corresponding to a vertical coordinate range relative to the tokamak equatorial plane: $z = -(13 \pm 1)$ cm ($r/a \approx 0.55$), $-(17 \pm 1)$ cm ($r/a \approx 0.75$), $-(21.5 \pm 1)$ cm ($r/a \approx 0.95$). *1* — Tokamak vacuum chamber, *2* — probing axis (probing from bottom to top), *3* — SR collection system mounting rail, *4* — lens, and *5* — slots for light guides. Angle $\alpha = 13.5^\circ$. *b* — Layout of optical fibers at the input (right) and output (left) of fiber bundles. The numbers of light guides are indicated in circles.

vertically is the optimum option. The output configuration of the fiber optic assembly is determined by the shape of the photosensitive region of a detector. The avalanche photodiode used in the circuit has a circular photosensitive region.

To reconstruct T_e based on the results of measurements of the scattered radiation spectrum with the TDC, one needs to perform relative calibration, which consists in finding the ratio of responses to radiation of a known spectrum of different spectral channels of the instrument. This relative calibration of TDC instruments was carried out using a SIRSH-8.5-200 photometric lamp, which has a radiation spectrum close to that of a blackbody. The electron temperature is reconstructed by searching for the best fit between the ratios of experimental values of SR signals in the polychromator channels and the synthesized values obtained using a formula characterizing the Thomson scattering spectrum with relativistic corrections [3]. The least squares method with statistical weights described in [4] is used for this purpose. The formula for the scattering signal measurement error was taken from [1], and the theory underlying the diagnostics is outlined in [5].

This paper presents the results of application of the above-described TDC in the examination of the T_e evolution shot-to-shot in ohmic discharges on the TUMAN-3M tokamak in two scenarios: a transition to the ohmic H-mode initiated by an increase in the working gas (deuterium) puffing rate, which is a method often used at this tokamak (see, e.g., [6]), and a scenario with modulation of the working gas puffing (WGP) rate in hydrogen plasma.

The T_e measurements in the described experiments with the L–H-transition were carried out at the following discharge parameters: plasma current $I = 150$ kA, toroidal field on the chamber axis $B_{tor} = 1$ T, and plasma density (measured using a 2-mm interferometer along the central chord) $\bar{n}_e \sim (1.3{-}2.9) \cdot 10^{19}\,\mathrm{m}^{-3}$. Figure 2, *a* presents the results of electron temperature measurements in discharges of this scenario, the evolution of electron density $\bar{n}_e(t)$, and the data obtained in T_e measurements by the shot-to-shot method with a probe located in the $\rho = 1$ region. Figure 2, *b* shows the temporal evolution of the D_α line

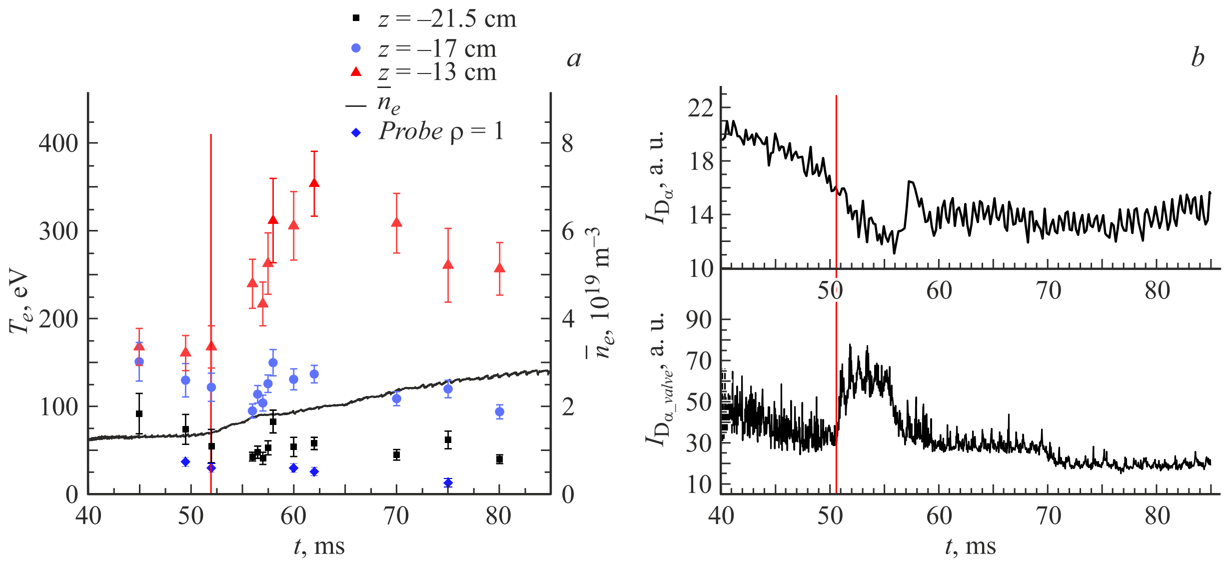

Figure 2. *a* — Temporal variation of the electron temperature at three spatial points in the H-mode measured by the Thomson scattering method, temporal evolution of the electron temperature according to the probe data in the $\rho = 1$ region, and evolution of chord-average density $\bar{n}_e(t)$ measured along the central chord of the interferometer. *b* — Intensity D_α proportional to the flux of deuterium atoms from the chamber wall (I_{D_α}) and the flow of working gas from the puffing system ($I_{D_{\alpha\_valve}}$). Vertical lines in panels *a* and *b* indicate the onset of the density increase and gas puffing, respectively.

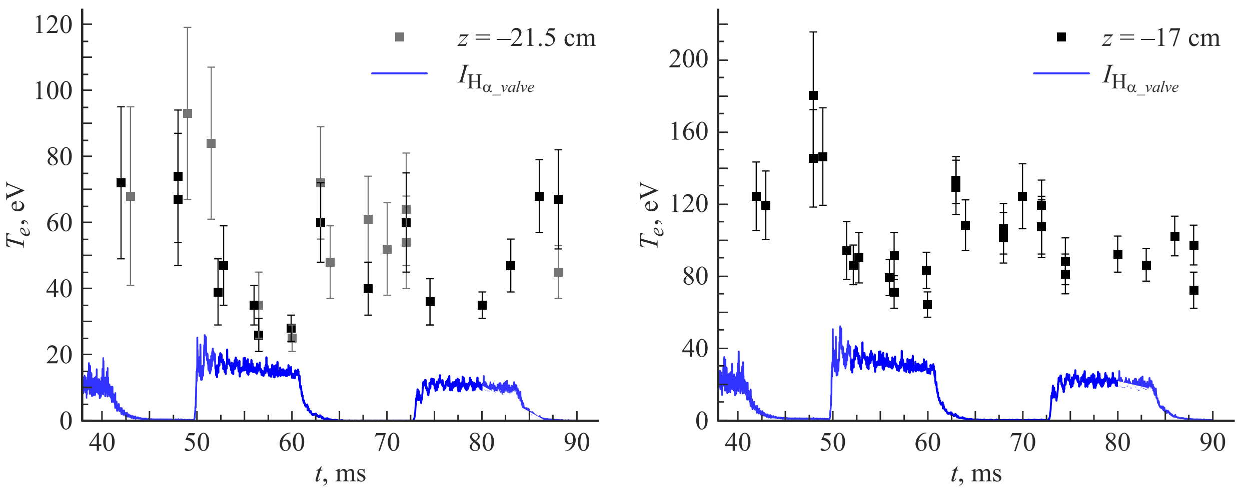

Figure 3. Temporal variation of the electron temperature in edge plasma in the experiments with gas puffing modulation at spatial points with $z = -21.5$ cm (the local n_e value varied within the range of $(0.21-0.45) \cdot 10^{19}\,\mathrm{m}^{-3}$) and $z = -17$ cm (the local n_e value varied within the range of $(0.75-1.39) \cdot 10^{19}\,\mathrm{m}^{-3}$). $I_{H_{\alpha\_valve}}$ — H_α intensity proportional to the flow of working gas from the puffing system.

emission intensity measured in two different regions: near the WGP valve ($I_{D_{\alpha\_valve}}$) and in a chamber section remote from the WGP valve (I_{D_α}).

It can be seen from Fig. 2, *b* that the rate of deuterium inflow increases within the time interval of 51–56 ms, and $\bar{n}_e$ starts increasing approximately at 52 ms. When the WGP is turned off, the plasma density continues to increase, although the particle source is smaller than before. This is indicative of an improved particle confinement in the tokamak. It can be seen from Fig. 2, *a* that the electron temperature at spatial point $z = -13$ cm increases significantly (from 160 to 350 eV) after 55 ms, while the temperature at spatial points $z = -17$ and -21.5 cm varies little. The pronounced T_e gradient enhancement seen in Fig. 2 is indicative of the formation of a transport barrier that suppresses the heat transfer between spatial points $z = -13$ and -17 cm. A steep electron temperature gradient in this region has already been observed at the TUMAN-3M tokamak (see [7]) in measurements performed with the TDC that existed until 2002. Note that point $z = -21.5$ cm could not be probed in these earlier experiments [7]. There is no reason to associate the temperature growth in this region with an increase in power input accompanying the increase in deuterium puffing rate within the time interval of 50–55 ms, since the loop voltage decreases from 3 to ~ 2.25 V within this interval at a almost constant plasma current.

In the WGP rate modulation mode, the electron temperature was measured in discharges with the following parameters: $I = 150$ kA, toroidal field on the chamber axis $B_{tor} = 1$ T, and $\bar{n}_e \sim (1.4-2.2) \cdot 10^{19}\,\mathrm{m}^{-3}$. The results of electron temperature measurements in this mode are shown in Fig. 3. The local values of n_e indicated in the caption to Fig. 3 were obtained by reconstructing the $n_e(r)$ profiles along the interferometer chords. It can be seen from Fig. 3 that T_e in edge plasma decreases after the WGP is turned on and increases after the gas puffing is completed. This is in line with simple theoretical considerations: an increase in the density of cold neutral particles leads to an increase in energy losses due to line emission of neutral hydrogen, dissociation, and electron-impact ionization of gas supplied from the puffing system. The ratio of the useful (scattered) radiation intensity to the intensity of parasitic radiation scattered from the chamber walls turned out to be lower in this series of discharges. In the gas puffing modulation mode, the useful scattering signal was significantly weaker than in the H-mode experiments, since the plasma density was low. In addition, a high intensity of stray radiation (presumably, due to particle contamination of glasses) was observed in discharges with gas puffing modulation. The reduced signal-to-noise ratio led to an increased error of temperature measurements.

Thus, the test scheme of the commissioned diagnostic complex was found to be efficient and sufficiently sensitive. It also enabled us to carry out previously impossible measurements of the electron temperature in edge plasma at the TUMAN-3M tokamak. The range of reliably measured temperatures was 20–360 eV (T_e up to 800 eV in the central plasma region were measured later) with an average relative error of no more than 10% at density $n_e = (0.2-2) \cdot 10^{19}\,\mathrm{m}^{-3}$. Following the studies described above, the used scattered radiation collection system was replaced with a upraged one that includes a lens optimized for operation in the TUMAN-3M tokamak TDC and a cassette for fiber optic bundles, which allows for rapid moving of fiber assemblies between slots, opening up the possibility of examining the electron temperature profile by the shot-to-shot method. Absolute calibration of the TDC, which will enable the measurement of local electron density values, is being planned at the moment.

Acknowledgments

The authors wish to thank their colleagues at Spectral Tech who designed and constructed the spectrum analysis complex used in this study.

Funding

The Thomson diagnostic complex used in this paper was constructed with financial support of state assignment FFUG-0021-0001; experiments were supported by state assignment FFUG-0024-0028.

Conflict of interest

The authors declare that they have no conflict of interest.

References

[1] G.S. Kurskiev, Al.P. Chernakov, V.A. Solovey, S.Yu. Tolstyakov, E.E. Mukhin, A.N. Koval, A.N. Bazhenov, S.E. Aleksandrov, N.S. Zhiltsov, V.A. Senichenkov, A.V. Lukoyanova, P.V. Chernakov, V.I. Varfolomeev, V.K. Gusev, E.O. Kiselev, Yu.V. Petrov, N.V. Sakharov, V.B. Minaev, A.N. Novokhatsky, M.I. Patrov, A.V. Gorshkov, G.M. Asadulin, I.S. Bel'bas, Nucl. Instrum. Meth. Phys. Res. A, **963**, 163734 (2020). DOI: 10.1016/j.nima.2020.163734

[2] N.S. Zhiltsov, G.S. Kurskiev, E.E. Mukhin, V.A. Solovey, S.Yu. Tolstyakov, S.E. Aleksandrov, A.N. Bazhenov, Al.P. Chernakov, Nucl. Instrum. Meth. Phys. Res. A, **976**, 164289 (2020). DOI: 10.1016/j.nima.2020.164289

[3] A.C. Selden, Phys. Lett. A, **79**, 405 (1980). DOI: 10.1016/0375-9601(80)90276-5

[4] T.Yu. Akatova, S.G. Goncharov, G.T. Razdobarin, A.N. Shil'nikov, *Chislennoe modelirovanie eksperimenta po diagnostike plazmy metodom tomsonovskogo rasseyaniya* (Fiz.-Tekh. Inst., L., 1986) (in Russian).

[5] V.V. Bulanin, *Diagnostika vysokotemperaturnoi plazmy* (Izd. Politekh. Univ., SPb., 2008), pp. 115–130 (in Russian). DOI: 10.18720/SPBPU/2/si20-186

[6] S.V. Lebedev, L.G. Askinazi, F.V. Chernyshev, M.A. Irzak, V.A. Kornev, S.V. Krikunov, A.D. Melnik, D.V. Razumenko, V.V. Rozhdestvensky, A.I. Smirnov, A.S. Tukachinsky, M.I. Vild'junas, N.A. Zhubr, Nucl. Fusion, **49**, 085029 (2009). DOI: 10.1088/0029-5515/49/8/085029

[7] A.S. Tukachinskii, *Elektronnyi balans v rezhimakh s uluchshennym uderzhaniem pri omicheskom nagreve plazmy v tokamake TUMAN-3M*, Candidate's Dissertation in Mathematics and Physics (Fiz.-Tekh. Inst. im. A.F. Ioffe, SPb., 2008) (in Russian).

Translated by D.Safin